Lasers in Manufacturing Conference 2023

Investigation of process improvements through laser preheating in extrusion-based additive manufacturing process

Dennis Meisner[a,*], Lukas Forstner[a], Nikitas Kaftiranis, Stefan Hierl

[a]*Laser Material Processing Laboratory, Ostbayerische Technische Hochschule Regensburg, Am Campus 1, 92331 Parsberg, Germany*

Abstract

Fused layer modeling (FLM) is widely used and is gaining more acceptance in the industry mainly due to its material variety and low costs. However, the usage is limited by a process-related anisotropy of the produced parts. The strength and ductility of the printed parts are significantly lower in the build-up direction than perpendicular to it. This is caused by insufficient interlayer bonding resulting from a reduced surface temperature in the process zone. To overcome this problem, a diode laser is integrated into the conventional FLM process to increase the surface temperature between the already printed surface and the newly applied substrate directly at the deposition zone. The investigations carried out show a significant improvement in the mesostructure, as well as a clear reduction in the anisotropy of the printed test specimens.

Keywords: fused layer modeling; laser preheating; anisotropy; interlayer bonding; mesostructure

1. Introduction

Due to its large material variety and low costs the extrusion-based additive manufacturing process Fused Layer Modeling (FLM), also known as Fused Filament Fabrication (FFF) or Fused Deposition Modelling (FDM), enables a wide range of applications in various industries [1]. The process is based on the extrusion of molten thermoplastic material along a pre-determined path. Each strand of material solidifies upon contact with the previously applied substrate. A layer-by-layer Deposition of multiple strand elements creates a three-dimensional object [2].

As the material is deposited, solidification occurs quickly due to the small thermal mass. This leads to insufficient reheating of the underlying substrate. Low temperatures in the bonding zone result in reduced molecular mobility, and lastly, can result in weak adhesion between the layers. Consequently, the mechanical properties of FLM-manufactured components in the build-up direction Z (perpendicular to the

build platform) deviate strongly from those in the manufacturing X-Y-plane, as shown in Figure 1. In order to handle the anisotropic behavior, there are different approaches to increase the temperature of the bonding zone. Probably the most common solution is to increase the ambient temperature using an enclosure heater [3]. Other approaches are using hot air [4], infrared radiation [5], microwaves [6] or surface heating units [7] to increase the temperature of the underlying layer. This paper focuses on the approach to increase the contact temperature by laser preheating. For this purpose, a conventional FLM printer is equipped with a fiber-coupled diode laser and an off-axis optic, guaranteeing the preheating of an area immediately before material deposition. Tensile tests demonstrate the advantages of laser preheating in terms of anisotropy. Investigations of the fragments suggest better layer adhesion due to better interdiffusion of the macromolecules. Microtome sections are used to identify the influence on the internal part structure (mesostructure).

2. Anisotropy of the FLM process

The anisotropic properties of FLM-manufactured components are based on the strand-by-strand and layer-by-layer build-up strategy during manufacturing. A detailed analysis of the deposition process of a strand element shows that a hot strand is always applied to an already-cooled surface. Figure 1 illustrates the material application which can be divided into an extrusion, a bonding, and a consolidation phase [8].

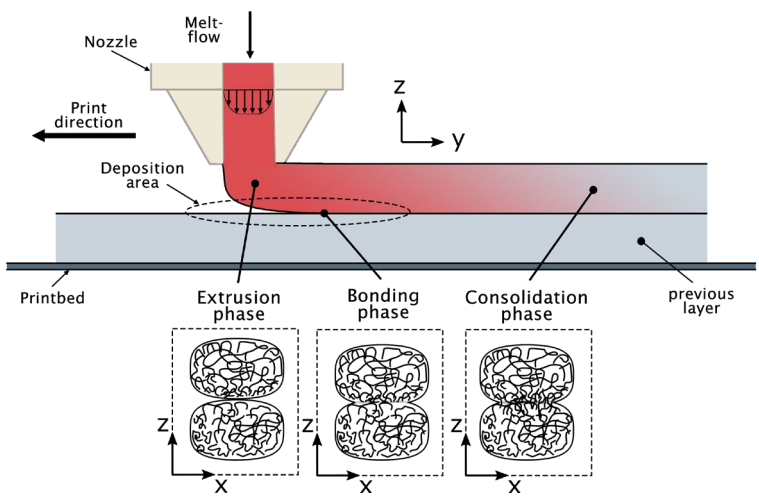

Fig. 1. Illustration of the material application in the FLM process, where a hot plastic melt is always applied to an already cooled previous layer. The application process is divided into an extrusion, a bonding, and a consolidation phase. In the bonding phase, the interdiffusion of macromolecules takes place.

In the extrusion phase, plastic filament is heated and forwarded to the deposition area via a nozzle usually with diameters of 0.4 to 1.2 mm. Similar to the injection molding process, the extrusion through the nozzle leads to an alignment of the macromolecules in the flow direction [9–11]. This favors anisotropic behavior in the strand direction and creates a poor precondition for interlaminar entanglement.

In the bonding phase, the already printed surface is covered by the thermoplastic melt creating a contact surface [12]. The thermal energy at this interface is crucial for the interdiffusion of the macromolecules. Only at higher contact temperatures full mobility of the plastic molecules can be maintained [8, 12–15]. In the case of semi-crystalline plastics, crystallization onset during cooling can further limit molecule mobility [8].

Due to the low thermal mass, the already cooled surface cannot be properly reheated, resulting in insufficient bonding. The same applies to the bonding of two strands next to each other during the building process of a single layer. However, since the temperature gradient is lower with respect to the nearby strand, better adhesion is formed in this case. This leads to a higher adhesion within a layer than the layer adhesion between two layers [3].

In order to ensure sufficient bonding between the individual strands the contact temperature at the deposition area of the molten plastic has to be increased. However, increasing the extrusion temperature can have a positive effect on the layer adhesion, but can lead to material degradation [3, 16]. Thus a second heat source is required to increase the surface temperature right in front of the deposition of new material. There are different approaches for increasing the temperature of the deposition area. A common solution, which is also proposed by the VDI Guideline 3405 is the use of an enclosure heater to increase the ambient temperature. However, high ambient temperatures can cause warpage of the parts and cannot prevent anisotropy entirely [3]. Another approach is preheating by means of hot air [4], infrared radiation [5], microwaves [6] or surface heating units [7] above the print head, where positive results are mentioned. With the integration of a laser into the FLM process, the energy input can be controlled in a more dynamic and precise manner compared to the mentioned approaches, resulting in a more reliable process. In addition, the laser preheating approach does not require an enclosed chamber, making the process more scalable as well. The laser preheating concept has been described in various publications, all of them reporting significant improvements [11, 17–22].

3. Experimental setup and methodology

3.1 Experimental setup

To qualify the laser preheating, a fiber-coupled diode laser (λ = 980 nm, P_{max} = 20 W) is integrated into a conventional FLM process. The optical fiber (400 µm) is equipped with an off-axis optics based on a lens-tube system. As shown in Figure 2, the beam shaping relies on just a focusing lens to save weight to not affect the dynamics of the printer. The off-axis optic is aligned to focus the beam on the surface directly in front of the Nozzle (spot diameter 1.3 mm, distance from nozzle 2.9 mm). In this way, the strand (width approx. 0.45 mm) that is currently being applied, the strand beside, and the strand area of the next print path are exposed to the laser beam.

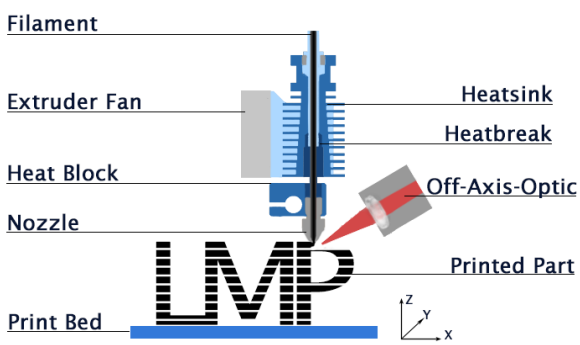

Fig. 2. Illustration of the laser-enhanced FLM process in which a fiber-coupled diode laser is integrated into the process to preheat the area immediately in front of the deposition area.

In the experimental design, the original form of the conventional FLM process was maintained. Thus, the original print head including the hotend (consisting of heatsink, heatbreak and heatbock with nozzle, etc.) is preserved. Figure 3 shows the final experimental setup on a Prusa i3 MK3S from Prusa Research. The printer is controlled by an OctoPrint Plugin, an Open-Source control and monitoring system running on a raspberry pi, where the laser is operated by embedded commands within G-Code.

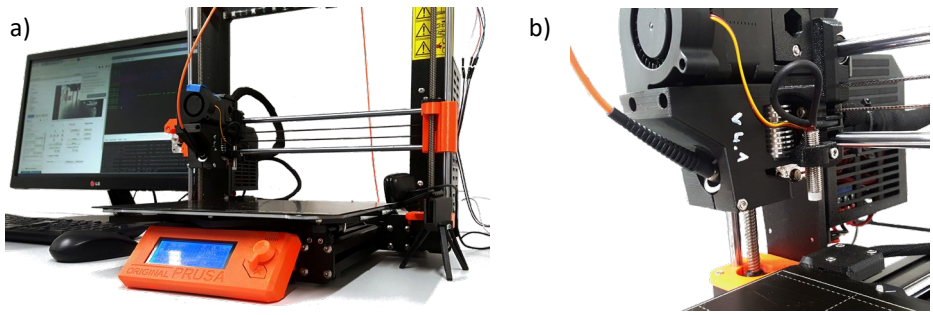

Fig. 3. (a) Final experimental setup based on a Prusa i3 MK3S printer from Prusa Research, equipped with off-axis optics for preheating the currently produced strand as well as the two strand areas beside the tool path. (b) Detailed view of the printhead equipped with a optics mount for the lens-tube system

3.2 Investigation Methodology

To evaluate the effect of laser preheating on the anisotropic behavior, tensile tests were performed to investigate the mechanical short-term behavior. For this purpose, both horizontal and vertical specimens are fabricated to evaluate the anisotropy. As shown in Figure 4, the test specimens are simple plates, since preheating using off-axis optics only allows manufacturing in one direction.

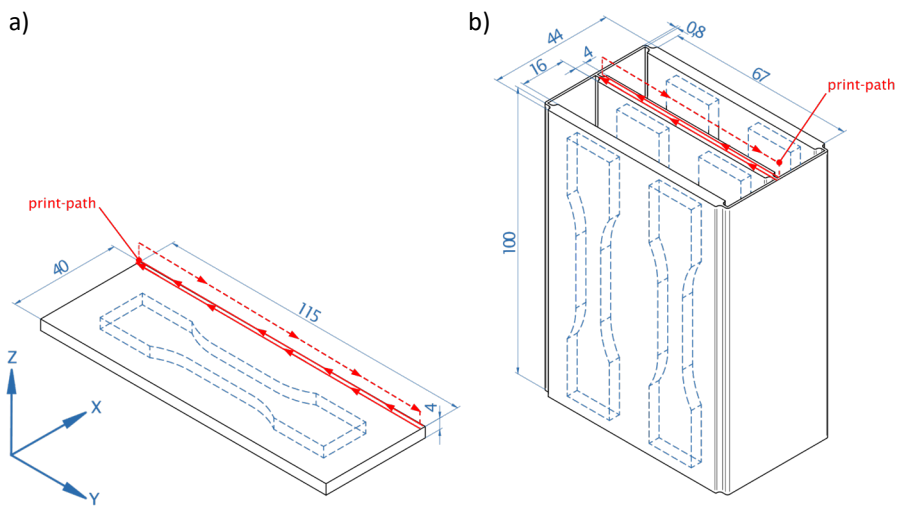

Fig. 4. Test specimens for mechanical investigation of the anisotropic behavior, as (a) horizontal and (b) vertical plates for tensile tests geometries (vertical plates as self-supporting structures, in order to avoid defects due to vibrations)

In order to investigate only the effect of preheating, the deposition of a single strand is combined with a return travel path above the manufacturing plane. For this, the G-code is adapted via a post-processing script, since the conventional infill is manufactured via a zig-zag pattern. The vertical plates are printed in a self-supporting geometry to avoid defects due to vibrations during the printing process. After printing, test specimens are cut out of the plates in a stationary area by means of a waterjet cutter. The stationary area is defined as domain with constant manufacturing parameters to ensure the printing speed is consistent. To reduce printing time and improve printability, a modified specimen geometry is used. The design is based on the Type-1A of DIN 527-2 with a shorter overall length, developed by SKZ (Süddeutsches Kunststoff-Zentrum). The modified geometry is considered unproblematic according to the original norm geometries [23]. All specimens are conditioned according to DIN EN ISO 291 for a non-tropical environment (23°C/50% rel. humidity) for at least 88 hours [24]. The tensile tests were performed on a Galdabini Quasar 100 universal testing machine following the DIN EN ISO 527 [25].

In order to further investigate the influence of laser preheating, a fracture surface examination of the fragments is performed. In addition, small rectangular-shaped specimens are used to analyze the mesostructure (internal structure of the part) by microtome sections. The preparation is performed in a stationary area of the samples. A microtome (Leica RM2255) is used to cut the thin slices to a width of about 30 µm, which are analyzed using an Olympus BX53M transmitted light microscope.

4. Results of the investigation

The laser preheating is verified using PLA (Prusament PLA Jet Black by Prusa Research). As the initial point for the process investigation, the slicer config "0.15 mm QUALITY MK3" (referred to Prusa Slicer) is chosen. Various print speed and laser power combinations were tested to explore suitable process parameters. With increasing laser power, a reduction of defects can be observed. At high laser powers (>7.5 W at 80 mm/s) the process becomes increasingly unstable and manifests itself in an accumulation of defects and in embrittlement of the material, which is caused by thermal degradation. In addition, defects or "cracks" near the print bed (z=0) are noticeable. Reducing the printing speed from 80 mm/s to 40 mm/s leads to a reduction of these.

The optimal parameter settings for PLA were determined at a laser power of 5.0 W with a print speed of 40 mm/s. Table 1 summarizes the process parameters used for the specimen preparation for mechanical testing. In order to qualify the influence of the laser, a comparison group is manufactured with the same process parameters, but without laser preheating.

Table 1. Process parameters for sample preparation

Process parameter	Unit	FLM		LE-FLM	
Orientation	-	horizontal	vertical	horizontal	vertical
Laser power	W	0.0		5.0	
Print speed	$\mathrm{mm/s}$	40.0		40.0	
Printbed temperature	°C	60		60	T_{amb}*
Nozzle temperature	°C	215			
Nozzle Ø	mm	0.4			
Layer height	mm	0.15			
Filament-Ø	mm	1.75			
Material	-	Prusament PLA Jet Black			
Number of test specimens	-	5	5	6	6

*T_{amb}:ambient temperature

In the tensile test, the characteristic values tensile strength σ_m, elongation at break ε_b, strain at tensile strength ε_m and the modulus of elasticity E_t are determined. These values are used to characterize the manufacturing-specific specimen behavior, allowing to evaluate the influences of laser preheating. Considering the results of the tensile tests in Fig. 5, a significant improvement of tensile strength σ_m and elongation at break ε_b in vertical orientation can be observed. The tensile strength is improved by 62% and the elongation at break by 67% with the help of laser preheating. However, the material behavior remains brittle and cannot reach the tensile strength of the specimens oriented horizontally.

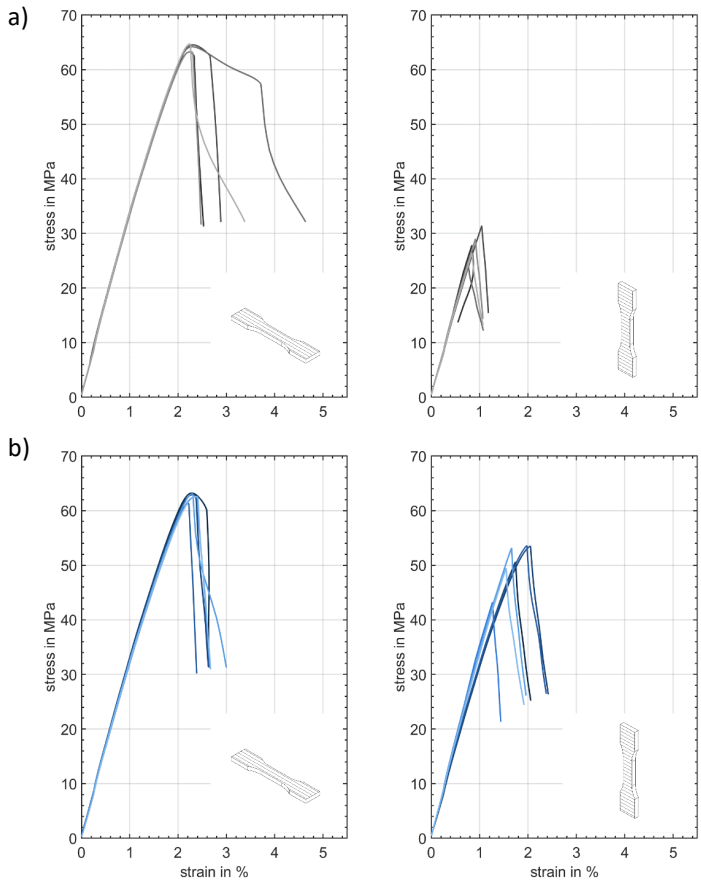

Fig. 5. Stress-strain curves of the specimens in a horizontal and vertical orientation without laser preheating (a) (5 specimens each) and (b) with laser preheating PG-02 (6 specimens each)

Comparing the horizontal orientation of the two test groups, the tensile strength of the laser-preheated specimens is slightly lower. This is also true for the elongation at break, although in the case of the preheated specimens, there is a smaller variance over all curves. In some cases, high elongation at break can be observed in the horizontally printed samples without preheating (Fig. 5a), although PLA is a less ductile material. This characteristic is not observed in the preheated test group.

An isotropy coefficient is used to evaluate the anisotropic properties within a test group. The coefficient indicates the ratio of the mechanical properties in build-up direction (Z-direction) to the corresponding properties parallel to the manufacturing plane (XY-plane). Thereby, a value of 0 is to be understood as

absolute anisotropic behavior and a value of 1 as an ideal isotropic material. Taking the tensile strength σ_m as an example, an isotropy coefficient of e.g. 0.5 indicates that the tensile strength in the Z-direction is 50% of the strength in the XY-plane. By visualizing the individual isotropy coefficients as an overall net-diagram (Figure 6), the influence of laser preheating on the anisotropic behavior can be shown.

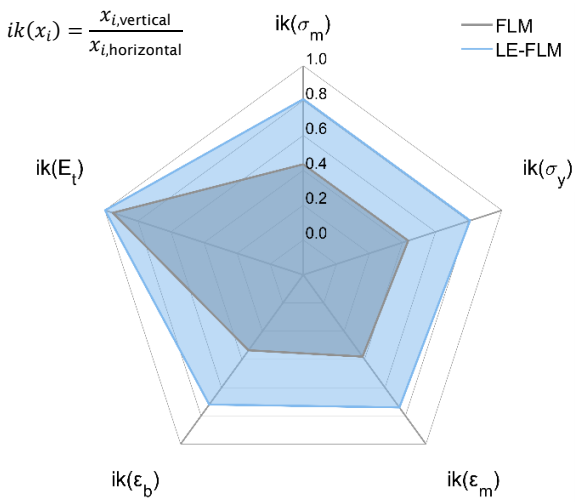

Fig. 6. Isotropy coefficients for the following mechanical properties: σ_m = tensile strength; σ_y = yield stress; E_t = tensile modulus; ε_m = elongation at tensile strength; ε_b = elongation at break.

Thereby, the isotropic coefficients represent the individual axes of the diagram. A fully filled area in the net-diagram would represent ideal isotropic behavior over all mechanical properties, determined at the tensile tests. Thus, an expansion of the enclosed domain can be interpreted as an optimization of the isotropic characteristics. The comparison of the conventional FLM process with the laser-enhanced (LE-)FLM method clearly shows a significant reduction of the process-related anisotropy.

With the help of an additional optical inspection of the fracture surfaces, especially of the vertical specimens, the effect of laser preheating can be further evaluated. The main goal of the optical analysis is the characterization of the layer bonding. A distinction between adhesion and cohesion fracture for the FLM and LE-FLM samples provides information about the functionality and effect of laser preheating. Figure 7 illustrates the different fracture types which can occur under vertical load perpendicular to the layer.

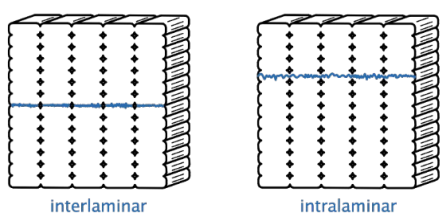

Fig. 7. Illustration of the fracture types which can occur under vertical load (perpendicular to the layer).

Adhesion or interlaminar fracture describes a failure between two layers or at the interface between two deposited filament strands. Cohesive or intralaminar fracture, on the other hand, describes a failure within a layer or a strand. To characterize the fracture surface and the internal mesostructure, two different perspectives are prepared, as shown in Figure 8. For this purpose, in the case of Fig. 8 a) a top view of the specimen is taken and in the case of Fig. 8 b) the fracture fragment is cut into pieces, embedded in epoxy resin, grounded, and polished. The mesostructure and fracture contour (at the top surface) are then analyzed under polarized light.

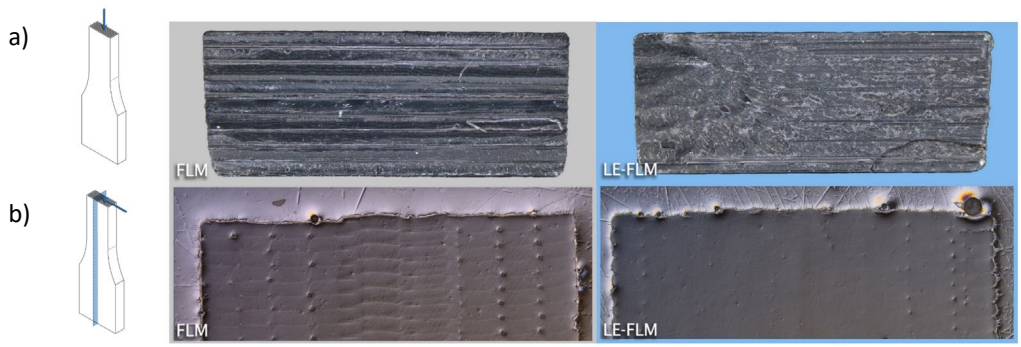

Fig. 8. (a) Top view of the fracture surface of vertical printed test specimens for the FLM process and the LE-FLM process (b) cross-section of the fracture surface (upper edge) and internal mesostructure based on a polished sample embedded in expoxy resin shown under polarized light for the conventional FLM process and the LE-FLM process

Looking at the fracture surface from above (Fig. 8 a), in the case of the conventional FLM process, the individual melt strands are visible and the fracture surfaces appear mostly smooth. This indicates that no sufficient bonding has occurred between the layers and the failure occurs merely interlaminar (adhesive) between the layers. A view of the fracture surface in cross-section (Fig. 8 b) confirms the described failure appearance from above. In case of the LE-FLM fracture fragments, the surfaces (Fig. 8 a) appear rougher, with the individual strand contours partially disappearing. This is noticeable through the lighter regions in the top view or the ragged fracture surface on top of the cross-section view (Fig. 8 b) and indicates improved interdiffusion between the macromolecules of the individual strands. Looking only at the mesostructure of the polished fragments (Fig. 8 b), a reduction of the defects can be observed. In addition, no strand pattern can be observed, resulting in a more homogeneous structure. The strand contour is only visible on the outer edges. This is caused by the manufacturing of the vertical specimens, as the outer perimeters were not exposed to the laser beam to protect the build plate. The additional investigation of the inner part structure by means of microtome sections once again shows the influence of the laser preheating on the mesostructure. Figure 9 shows two representative sections for the parameter setting mentioned above.

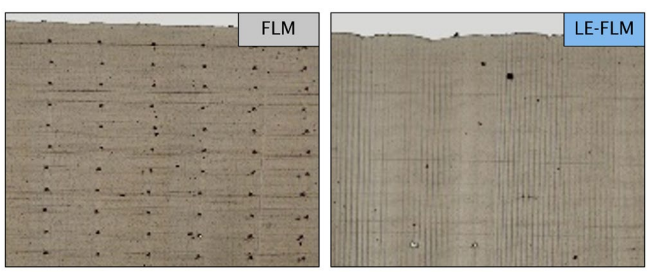

Fig. 9. Microtome section of test specimens for analysis of the mesostructure under transmitted light.

While in the conventional process, the strand pattern can be recognized by the defects at the corners, in the case of the LE-FLM no defect pattern is visible. In addition, a reduction of defects is detectable here as well. In case of the LE-FLM tin cuts, strand contours are difficult to recognize even by transmitted light. In vertical orientation, however, a layer pattern is slightly noticeable. This could be the reason why the anisotropic properties could not be eliminated completely. All in all, this confirms the positive influence of the laser on the mesostructure and the improved mechanical properties in build direction.

Both the mechanical and optical investigations indicate that the contact temperature in the deposition zone is essential for the interlayer bonding between the layers or strands. This leads to the assumption that the higher temperatures achieved by laser preheating led to better interdiffusion of the macromolecules.

5. Summary and Conclusions

The results of the investigation of the extrusion-based FLM process clearly show the existing process-related anisotropy and the improvements that can be achieved by laser preheating. For the experimental setup, a fiber-coupled diode laser was integrated into the conventional FLM process. Using an off-axis-optic, the area right in front of the deposition of new material was preheated during the manufacturing of test specimens. Tensile tests have shown an improvement in layer adhesion through laser preheating. Up to now an improvement of the tensile strength by 62% and the elongation at break by 67% was achieved in the building direction. The anisotropic behavior of printed parts can be improved significantly. Inspection of the fracture surface of the vertical printed tensile test specimens verifies the improvement through laser preheating. The preheating of the deposition zone leads to a different fracture behavior, which is shown by an intralaminar (cohesive) failure instead of an interlaminar (adhesive) failure. Furthermore, a significantly more homogeneous mesostructure can be observed, which can be explained by the laser preheating.

In order to validate these results, further mechanical tests must be carried out to verify the laser preheating. On the one hand, additional tensile tests of the adhesion between the strands within a layer must be carried out, and on the other hand, further materials have to be qualified. In addition, the temperature field in the deposition zone must be quantified and correlations to the process parameters must be established. This could lead to a further improvement in layer adhesion to achieve better isotropic material behavior.

References

[1] The State of 3D Printing (2022 Edition): Sculpteo.

[2] T. D. Ngo, A. Kashani, G. Imbalzano, K. T. Nguyen, and D. Hui, “Additive manufacturing (3D printing): A review of materials, methods, applications and challenges,” Composites Part B: Engineering, vol. 143, pp. 172–196, 2018, doi: 10.1016/j.compositesb.2018.02.012.

[3] Additive Fertigungsverfahren Gestaltungsempfehlungen für die Bauteilfertigung mit Materialextrusionsverfahren, VDI 3405 Blatt 3.4, VDI Verein Deutscher Ingenieure e.V., Berlin, Jul. 2019.

[4] H. Prajapati, S. S. Salvi, D. Ravoori, M. Qasaimeh, A. Adnan, and A. Jain, “Improved print quality in fused filament fabrication through localized dispensing of hot air around the deposited filament,” Additive Manufacturing, vol. 40, p. 101917, 2021, doi: 10.1016/j.addma.2021.101917.

[5] V. Kishore et al., “Infrared preheating to improve interlayer strength of big area additive manufacturing (BAAM) components,” Additive Manufacturing, vol. 14, pp. 7–12, 2017, doi: 10.1016/j.addma.2016.11.008.

[6] A. Andreu, S. Kim, J. Dittus, M. Friedmann, J. Fleischer, and Y.-J. Yoon, “Hybrid material extrusion 3D printing to strengthen interlayer adhesion through hot rolling,” Additive Manufacturing, vol. 55, p. 102773, 2022, doi: 10.1016/j.addma.2022.102773.

[7] J. W. H. Andreas, U. Popp, L. Pfotzer, B. Okolo, and M. T. Tran, “3D-Druckvorrichtung,” DE102015111504 (A1), DE DE201510111504 20150715, Jan 19, 2017.
[8] B. Brenken, E. Barocio, A. Favaloro, V. Kunc, and R. B. Pipes, “Fused filament fabrication of fiber-reinforced polymers: A review,” Additive Manufacturing, vol. 21, pp. 1–16, 2018, doi: 10.1016/j.addma.2018.01.002.
[9] Z. Zhao, X. Zhang, Q. Yang, T. Ai, S. Jia, and S. Zhou, “Crystallization and Microstructure Evolution of Microinjection Molded Isotactic Polypropylene with the Assistance of Poly(Ethylene Terephthalate),” Polymers, vol. 12, no. 1, 2020, doi: 10.3390/polym12010219.
[10] Z. Tadmor, “Molecular orientation in injection molding,” J. Appl. Polym. Sci., vol. 18, no. 6, pp. 1753–1772, 1974, doi: 10.1002/app.1974.070180614.
[11] P. Han, A. Tofangchi, A. Deshpande, S. Zhang, and K. Hsu, “An approach to improve interface healing in FFF-3D printed Ultem 1010 using laser pre-deposition heating,” Procedia Manufacturing, vol. 34, pp. 672–677, 2019, doi: 10.1016/j.promfg.2019.06.195.
[12] Q. Sun, G. M. Rizvi, C. T. Bellehumeur, and P. Gu, “Effect of processing conditions on the bonding quality of FDM polymer filaments,” Rapid Prototyping Journal, vol. 14, no. 2, pp. 72–80, 2008, doi: 10.1108/13552540810862028.
[13] A. Haufe and G. Mennig, “Untersuchung zur Vorhersage der Bindenahtfestigkeit in spritzgegossenen Formteilen,” Angew. Makromol. Chem., vol. 265, no. 1, pp. 75–81, 1999, doi: 10.1002/(SICI)1522-9505(19990301)265:1<75::AID-APMC75>3.0.CO;2-5.
[14] Sun, Qian (2005): Bond formation between polymer filaments in fused deposition modeling process. Master Thesis. University of Calgary.
[15] T. Nguyen-Chung, “Strömungsanalyse der Bindenahtformation beim Spritzgießen von thermoplastischen Kunststoffen,” Fakultät für Maschinenbau und Verfahrenstechnik, Technische Universität Chemnitz, Chemnitz, 2001.
[16] A. K. Sood, R. K. Ohdar, and S. S. Mahapatra, “Parametric appraisal of mechanical property of fused deposition modelling processed parts,” Materials & Design, vol. 31, no. 1, pp. 287–295, 2009, doi: 10.1016/j.matdes.2009.06.016.
[17] C. Kuehn, B. Nieseb, and G. Witt, “Verbesserung der mechanischen Eigenschaften im FLM-Verfahren durch lokale Laservorerwärmung und Endlosfaserverstärkung,” Rapid.Tech + FabCon 3.D International Hub for Additive Manufacturing: Exhibition + Conference + Networking, pp. 258–273, 2019, doi: 10.3139/9783446462441.019.
[18] J. Du, Z. Wei, X. Wang, J. Wang, and Z. Chen, “An improved fused deposition modeling process for forming large-size thin-walled parts,” Journal of Materials Processing Technology, vol. 234, pp. 332–341, 2016, doi: 10.1016/j.jmatprotec.2016.04.005.
[19] M. Luo, X. Tian, J. Shang, W. Zhu, and and D. Li, PEEK High Performance Fused Deposition Modeling Manufacturing with Laser In-Situ Heat Treatment.
[20] A. Deshpande, A. Ravi, S. Kusel, R. Churchwell, and K. Hsu, “Interlayer thermal history modification for interface strength in fused filament fabricated parts,” Prog Addit Manuf, vol. 4, no. 1, pp. 63–70, 2018, doi: 10.1007/s40964-018-0063-1.
[21] P. Han, A. Tofangchi, S. Zhang, A. Desphande, and K. Hsu, “Effect of in-process laser interface heating on strength isotropy of extrusion-based additively manufactured PEEK,” Procedia Manufacturing, vol. 48, pp. 737–742, 2020, doi: 10.1016/j.promfg.2020.05.107.
[22] A. K. Ravi, A. Deshpande, and K. H. Hsu, “An in-process laser localized pre-deposition heating approach to inter-layer bond strengthening in extrusion based polymer additive manufacturing,” Journal of Manufacturing Processes, vol. 24, pp. 179–185, 2016, doi: 10.1016/j.jmapro.2016.08.007.
[23] B. Gerets, T. Hochrein, and M. Bastian, Eds., Mechanisches Langzeitverhalten additiv gefertigter Kunststoffbauteile, 1st ed. Herzogenrath: Shaker, 2019.
[24] Kunststoffe - Normalklimate für Konditionierung und Prüfung (ISO 291:2008), DIN EN ISO 291, DIN Deutsches Institut für Normung e.V., Berlin, Aug. 2008.
[25] Kunststoffe - Bestimmung der Zugeigenschaften - Teil 2: Prüfbedingungen für Form- und Extrusionsmassen (ISO 527-2:2012), DIN EN ISO 527-2, DIN Deutsches Institut für Normung e.V., Berlin, Jun. 2012.